

Further Development of a High-Order Prediction Tool for Combustion at All Speeds

Foluso Ladeinde*

TTC Technologies, Inc., P.O. Box 1527, Stony Brook, NY 11790

The development of a high-order prediction tool presented in our earlier work on combustion is extended in the present paper. The approach predicts, at all Mach numbers, premixed, non-premixed, and partially-premixed turbulent combustion using large-eddy simulation (LES) combined with the level-set/mixture fraction laminar flamelet formulation. In the present work, we revisit the assumptions in our earlier efforts and expand the validation problems to include more results on the lean-premixed dump combustor and the V-gutter flame holder for aircraft engine. Agreement between the numerical results and the experimental data is obvious in most cases.

I. Introduction

The large-eddy simulation (LES) approach received increased attention from the combustion research community in recent years due to its potential to accommodate realistic engineering configurations and, unlike the Reynolds-Averaged Navier-Stokes (RANS) methods, accurately predict non-universal turbulent flow features. The aim of the numerical studies is to improve the understanding of the turbulence-chemistry interactions in complex configurations, such as partially-premixed flames.

In this paper, we consider the level-set method, which attempts to model the premixed flame from a geometrical point of view. Originally proposed by Williams,¹ the level-set equation, or G-equation, models the evolution of the flame front. Peters² proposed a transport equation for the level-set function treated as a distance function within the context of RANS. Pitsch and Duchamp de Lageneste,³ and later Pitsch,⁴ using LES, extended the level-set approach to include both the thin and corrugated flame regimes. Their numerical approach was based on a second-order spatial scheme, an improved model for the turbulent burning velocity. The mixing between the combustion products and the surrounding inert flow field was also modeled. Huang et al.⁵ considered the level-set approach and LES to study the combustion dynamics in a lean-premixed swirl-stabilized combustor. The LES equations were solved with a second-order finite volume method, while a flamelet library based on freely-propagating premixed flames was generated.

In the present work, based on a compressible formulation, we combine the level-set approach for premixed flame configurations with the conserved variable approach for non-premixed configurations. The combined model is similar to the approach used by Duchamp de Lageneste and Pitsch⁶ for a low-Mach number formulation. The ability of the model to capture partially-premixed flame characteristics is established by comparing the calculated results with those from available experiments.

The computational procedure in the present work is based on high-order spatial discretization of the governing equations. The compact, Padé approximant procedure⁷ is used for low-Mach number flows, and the weighted essentially non-oscillatory scheme⁸ (WENO) for high-Mach number flows. Thus, high-fidelity simulation is available at all speeds, from incompressible to supersonic or even hypersonic speeds. The high-order spatial discretization is matched in time by a fourth-order Runge-Kutta integration procedure. The node-implicit approach of Beam and Warming⁹ is also supported for time integration. In order to accommodate the analysis of realistic problems with complicated geometries and to be competitive with unstructured mesh methods, a matching high-order overset procedure was also developed and implemented.

* Director of Research, AIAA Life Member and Associate Fellow.

II. The Mathematical Models and Numerical Procedures

A. Numerical Approach for the Transport Equations

The fully compressible forms of the LES equations for continuity, momentum, and energy are employed in this study, as we are interested in the non-linear coupling between the acoustic, vorticity, and combustion fields. These equations are presented in our previous work.^{10,11} In order to facilitate the numerical simulation of flow configurations around arbitrary and complicated bodies, the transport equations are cast in the form of a generalized curvilinear coordinate system. These equations are implemented in AEROFLO, which is a multidisciplinary CFD software product developed by TTC Technologies, Inc. Various high- and low-order numerical schemes are available in this code for the discretization of the transport equations. For low-speed flows, a sixth-order accurate compact scheme is used. For high-speed flows, a fifth-order accurate WENO scheme is employed. For numerical simulations using lower-quality grids, a robust second-order MUSCL scheme is implemented. The details of the implementation of these schemes are presented in other works.¹¹

Due to the strong interaction between the flow field and the flame, accurate time-dependent solutions are required. To obtain this, either a second-order Beam and Warming algorithm⁹ or the classical fourth-order Runge-Kutta scheme in its low-storage form¹² is employed for time integration of the system of conservation equations.

B. The Laminar Flamelet Approach

In order to analyze premixed and partially-premixed reacting flows of practical interest, we couple the compressible formulation for the transport of mass, momentum, and energy, presented in the previous section, with a level-set methodology for premixed combustion. The level-set formulation is augmented with a mixture fraction approach for non-premixed combustion. The combined model allows for the modeling of flames through a flamelet approach that encompass all regimes: premixed, non-premixed, and partially-premixed. The main idea behind the flamelet approach, which is used to calculate the effects of chemical heat release on the flow field, is the assumption that a turbulent flame is a collection of laminar flamelets embedded in an otherwise inert turbulent flow. The flame inner structure can be calculated independent of the turbulent flow, using arbitrary detailed kinetic models and realistic multi-species transport properties.

The level-set methodology is described in detail in our previous work.¹⁰ High-order ENO spatial finite differences¹³⁻¹⁵ are coupled with second- and third-order total variation diminishing (TVD) Runge-Kutta schemes for time integration of the level-set transport equation. The distance function property of the level-set is enforced through a re-initialization procedure. For this purpose, we use the procedure of Sussman et al.,¹⁶ with the extension in Russo and Smereka.¹⁷

The conserved scalar or mixture fraction, Z , is related to the fuel-to-oxidizer equivalence ratio, Φ , as

$$Z = \frac{\Phi}{\left(\Phi + \frac{1 - Z_{st}}{Z_{st}} \right)}. \quad (1)$$

By convention, the conserved scalar, Z , will be called the mixture fraction throughout the rest of the paper, and Z_{st} , its stoichiometric value, which occurs when $\Phi=1$. The filtered LES equation for the Favre-filtered mixture fraction,⁶ solved using an approximate factorization technique similar to the one used by Spalart and Allmaras¹⁸ for the solution of their transport equation for turbulent viscosity, is employed here for the solution of the mixture fraction transport equation. The variance of the mixture fraction field, $\overline{Z'^2}$, is computed using the scale-similarity model of Cook and Riley.¹⁹

The partially-premixed combustion regime is a combination of the premixed and non-premixed reaction regimes. It occurs when both fuel and oxidizer are in excess in various premixed regions. The reactants left unconsumed in these regions can diffuse towards each other and, if conditions are right, ignite and lead to non-premixed flames. In order to model this regime, both premixed and non-premixed flamelet tables are necessary. Figure 1 shows a schematic for a lifted turbulent flame. This is a typical partially-premixed configuration featuring both premixed and non-premixed flame regions. In this figure, G corresponds to the level-set field and Z to the mixture fraction field. The fuel jet and the oxidizer coflow are mixing with each other. Premixed flame regions are established at some length downstream of the nozzles, highlighted in blue in the figure below. Behind these premixed regions, non-premixed flames, highlighted in red, are established between the fuel and the oxidizer streams.

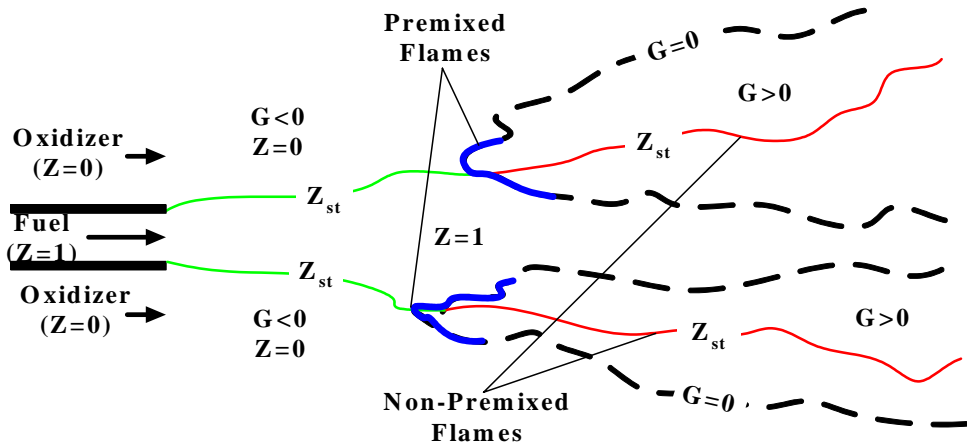


Figure 1 Schematic of a lifted turbulent flame.

For level-set values $G < 0$, the effect of the chemical reaction is modeled using the premixed flamelet table for the appropriate equivalence ratio (mixture fraction) value. For $G \geq 0$, both the premixed and non-premixed flamelet tables are used. For this case, the greater of the premixed and non-premixed source terms is chosen. As can be seen in Figure 1, the source term due to the premixed flame conditions will be significant only in the vicinity of the $G=0$ surface. At locations farther downstream, the non-premixed term is dominant.

III. Results

The numerical procedures described in the previous section have been implemented into AEROFLO. The aim of the combined high-order LES/level-set/mixture fraction approach is to accurately predict transient flame phenomena for partially-premixed flames and the detailed coupling between flow and combustion instabilities. The results presented here correspond to premixed flames with both uniform and variable equivalence ratios.

A. Flamelet Library

The schematics for freely propagating premixed flame (FPPF) and opposed jet flames are shown in Figure 2, while the calculation procedure for FPPF is shown in Figure 3. Sample filtered formation enthalpy, \tilde{H}_f^0 , data corresponding to the premixed flame table are shown in Figure 4. In this figure, $G=0$ corresponds to the flame surface, defined as the location of the peak heat release rate. The filtering process results in a multi-dimensional table such that the filtered formation enthalpy is a function of the distance to the flame surface, equivalence ratio (through the mixture fraction), grid size, mixture fraction variance, and flame stretch rate.

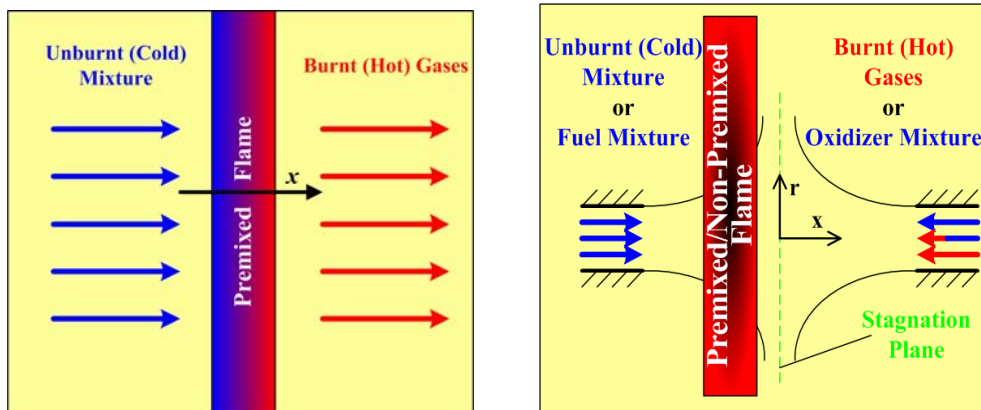


Figure 2 Schematic of the freely propagating (premixed) and opposed (non-premixed) jet flame.

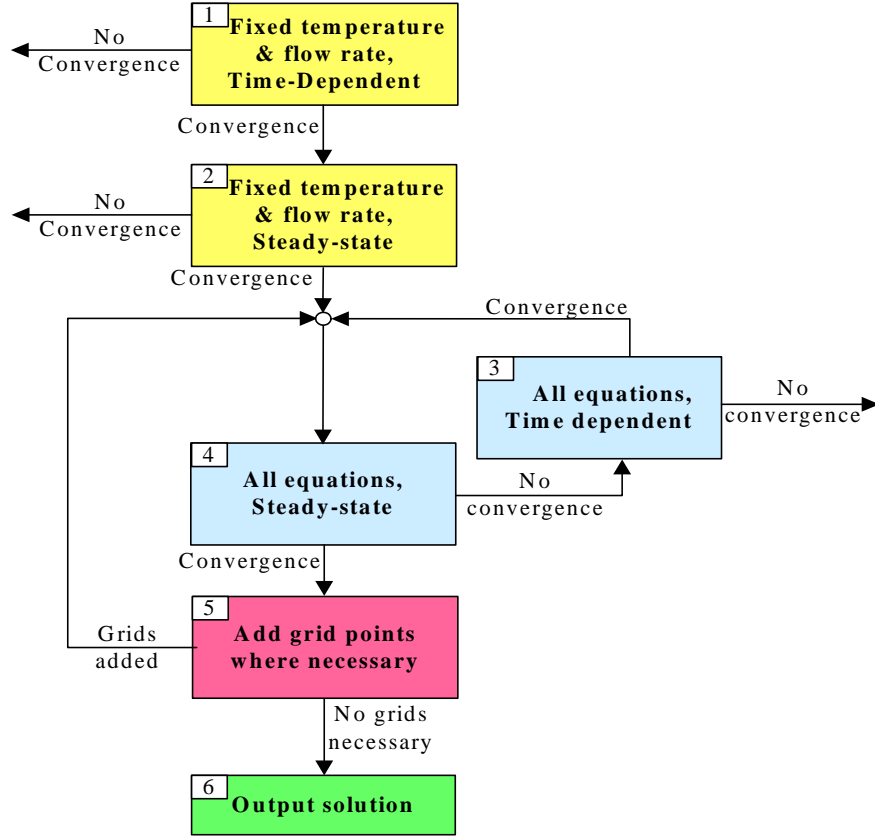


Figure 3 Chart for the FPPF iterative algorithm.

In order to save computational resources, the flamelet library is constructed prior to the start of the LES simulation. The range of values for each independent variable is chosen according to the values of characteristic parameters for the numerical simulation. The values for the signed distance to the flame are set large enough to ensure the entire flame is contained in the table. The set of equivalence ratio values covers the range $[\Phi_{min}, \Phi_{max}]$ corresponding to the experimental conditions, while the stretch rate values are set in the range $[0, K_{ext}]$, where K_{ext} is the extinction strain rate. The grid size, Δ , and mixture fraction variance, $\overline{Z''^2}$, become independent variables for the flamelet library since they appear as parameters in the PDFs for G and Z . Solutions are generated for several grid size values, $\Delta_{min} < \Delta < \Delta_{max}$, and mixture fraction variance values, $0 < \frac{\overline{Z''^2}}{\tilde{Z}(1-\tilde{Z})} < 1$. Here, Δ_{min} and Δ_{max} are the minimum and

maximum grid sizes, respectively, for a computational mesh. During the simulation, the values of the filtered formation enthalpy are extracted from the flamelet table through a multidimensional linear interpolation. The interpolation algorithm is designed to accommodate tables based on arbitrary numbers of independent variables. The procedure adapts automatically to cases where one or more independent variables are neglected (e.g., flame with constant equivalence ratio and/or $K=0$).

The results shown in Figure 4 correspond to stretch-free, $K=0$, methane-air flames computed using the detailed kinetic model GRI-Mech 3.0.²⁰ The peak negative formation enthalpy occurs near the stoichiometric mixture fraction value, which corresponds to $\tilde{Z} \approx 0.055$. Heat release and temperature solutions for the canonical combustion problems in Figure 2 are shown in Figures 5 and 6. Contour maps of the heat release in bluff body flame, temperature and vorticity in Bunsen burner flame and in V-gutter flames are shown in Figures 7, 8, and 9, respectively. The computational grid for an engine combustor that is currently being investigated with our procedure is shown in Figure 10.

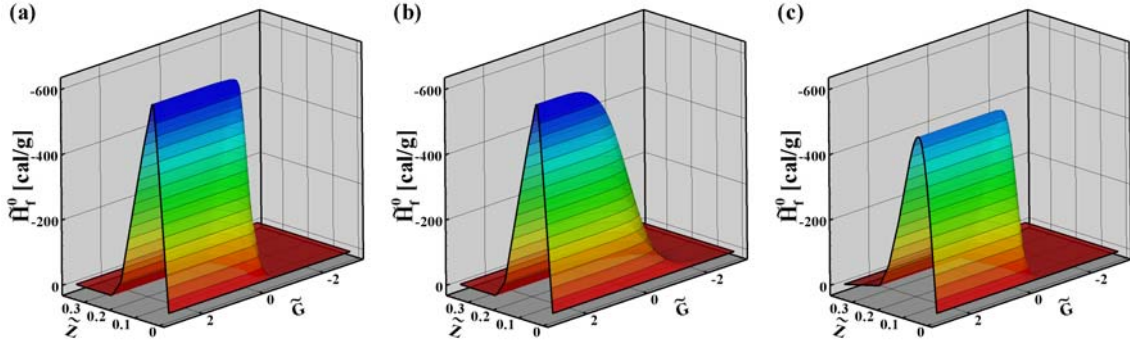


Figure 4 Sample \tilde{H}_f^0 values for methane-air flame at various values of the equivalence ratio. The filter width in the G-direction corresponds to $\frac{\Delta}{L_{ref}} = 0.003$ for (a) and (c) and to $\frac{\Delta}{L_{ref}} = 0.1$ for (b). For (a) and (b), the mixture fraction variance is $\frac{\overline{Z'^2}}{\overline{Z}(1-\overline{Z})} = 10^{-4}$, while for (c), $\frac{\overline{Z'^2}}{\overline{Z}(1-\overline{Z})} = 10^{-2}$. For this configuration, $L_{ref}=3cm$ and $K=0$.

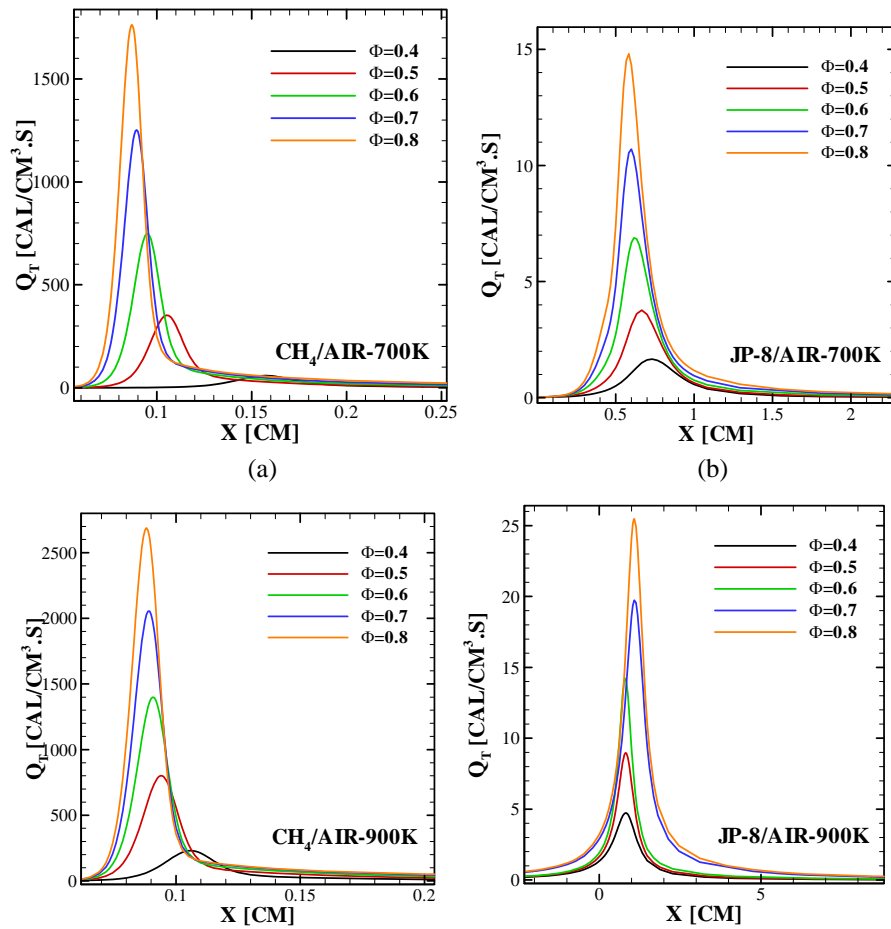


Figure 5 Heat release rate profiles for freely propagating premixed flames: (a) methane/air and (b) JP-8/air.

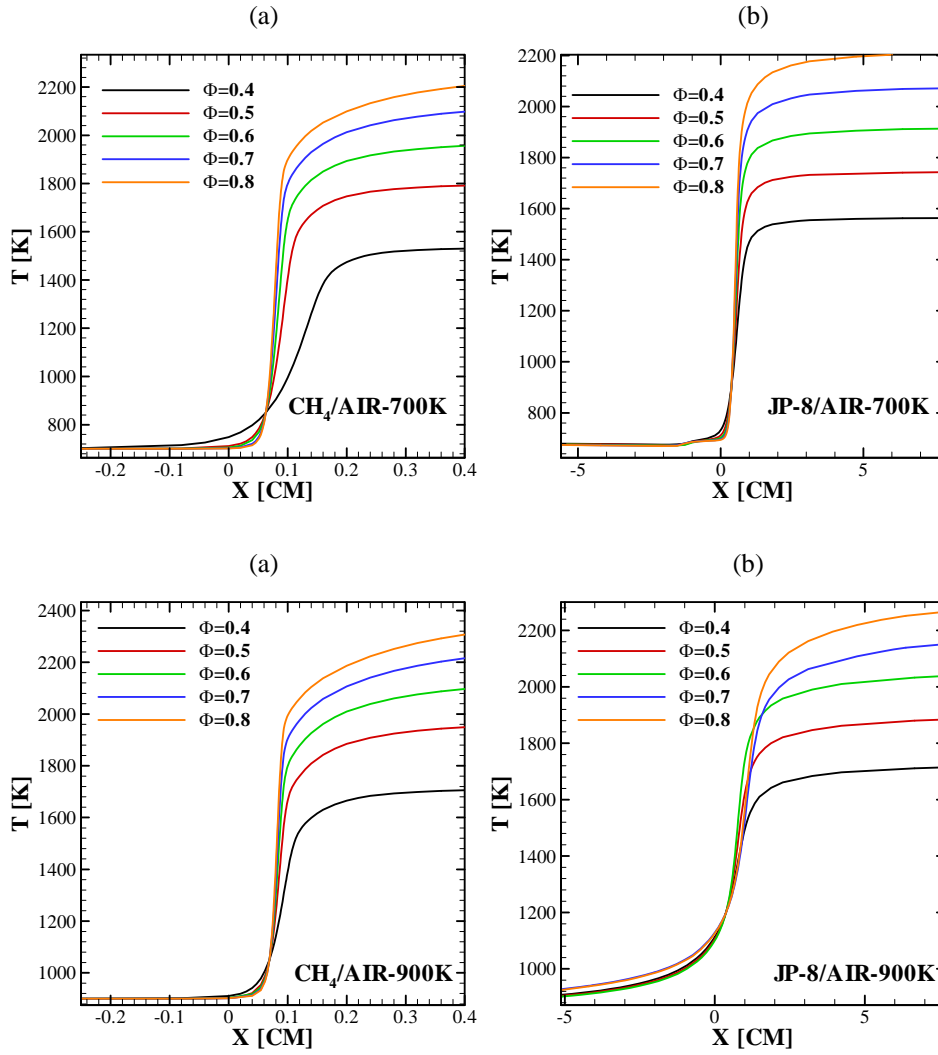


Figure 6 Temperature profiles for freely propagating premixed flames: (a) methane/air and (b) JP-8/air.

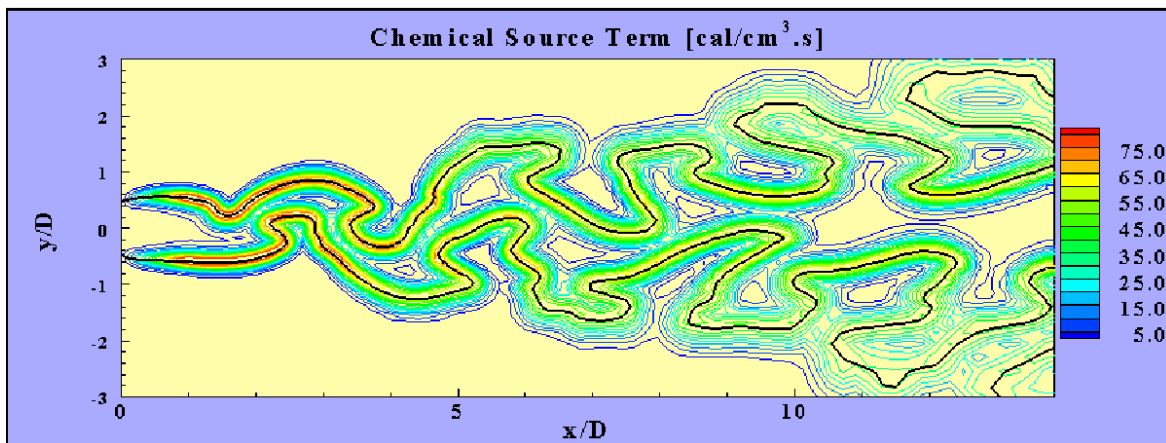


Figure 7 Volumetric heat release contour for bluff body flame.

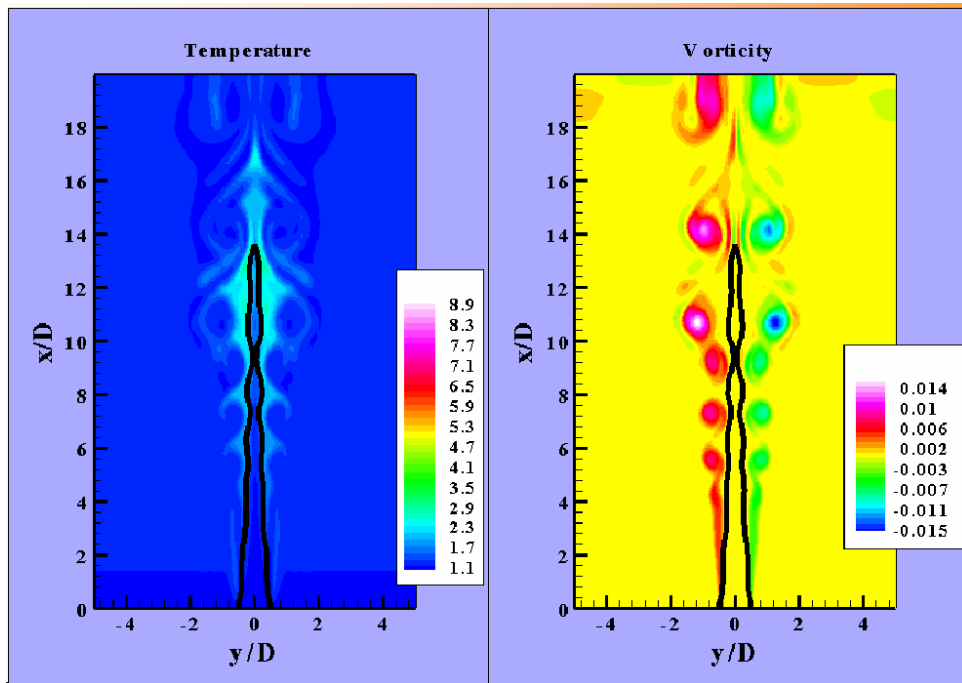


Figure 8 Contour map of Bunsen-burner flame.

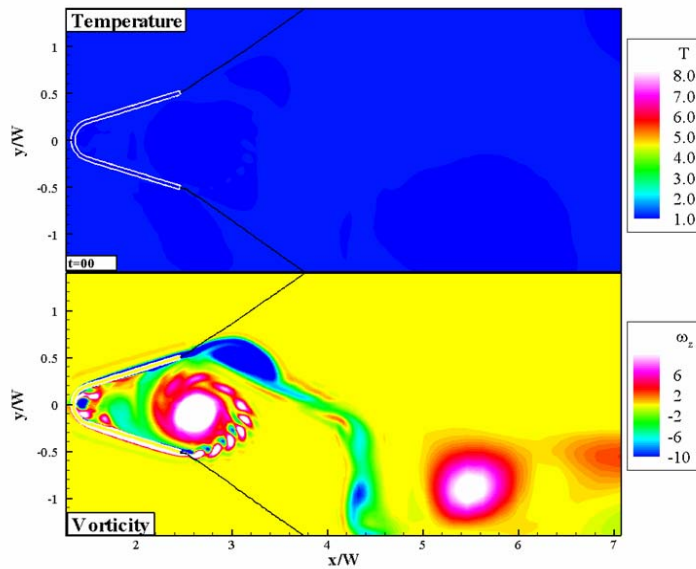


Figure 9 Temperature and vorticity map for V-gutter flame

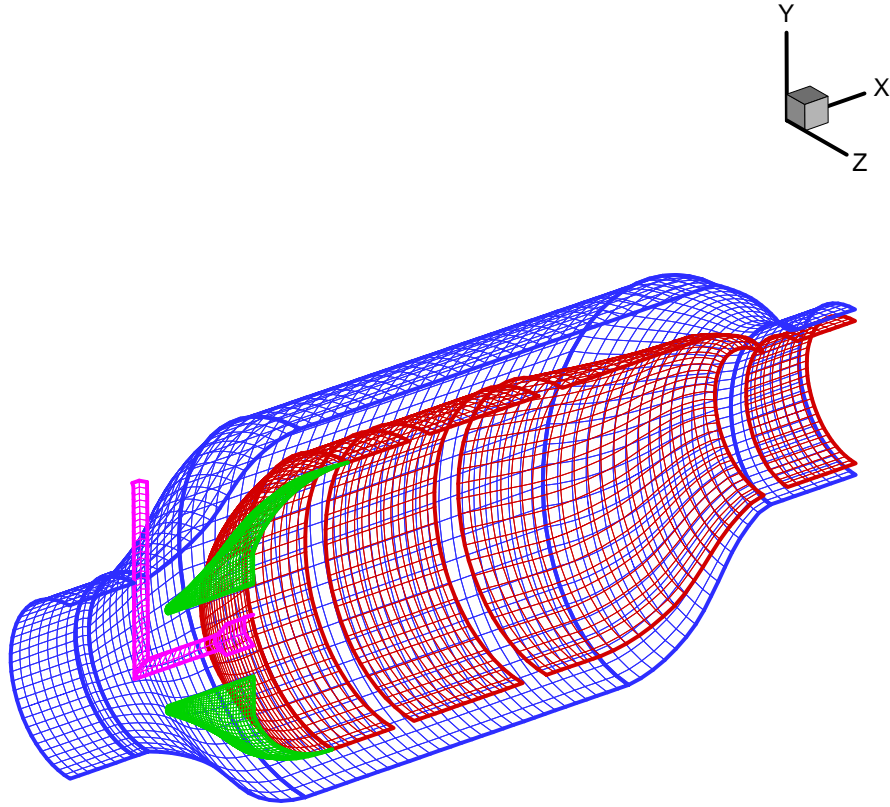


Figure 10 AEROFLO model for engine combustor.

B. Partially-premixed results

The Oracles experimental rig²¹ (Figure 11) is used to test the ability of the level-set/mixture fraction/flamelet formulation to capture the effects of variable equivalence ratios on the flow and combustion characteristics. This experimental configuration has been specifically developed to provide accurate test data for variations in the combustible mixture composition. The setup consists of two fully-developed turbulent channel flows that are emerging just before a sudden expansion. The flame is stabilized by the recirculation regions that occur behind each backward facing step. Figure 1 shows the six-block, two-dimensional computational grid used to perform non-reacting and reacting simulations for this configuration. The computational domain spans $7H$ upstream of the channel expansion into the combustion chamber. The length of the combustion chamber was set to $20H$. This size ensures that the average flame surface is entirely contained in the computational domain. The Reynolds number in the numerical simulation is set to match the experimental conditions, $Re=25,000$.

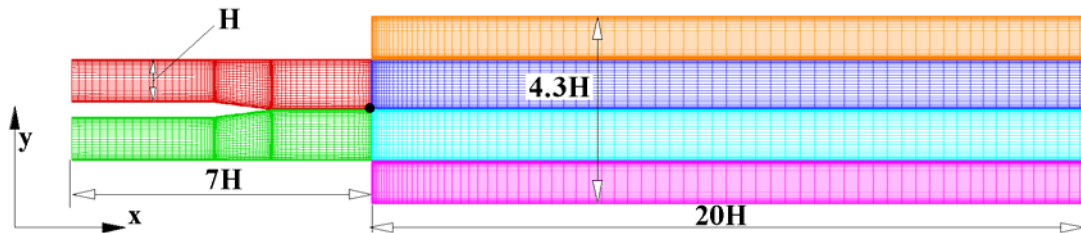


Figure 11 Computational grid used for the LES of lean dump combustor. The “dot” shows the origin of the physical coordinate system.

This configuration was also used by Duchamp de Lageneste and Pitsch⁶ to test the level-set model in their LES procedure for partially-premixed combustion in a low-Mach number flow. Our objective is to test the ability of a

level-set/mixture fraction flamelet approach, coupled with a high-order, fully compressible flow solver, to capture the variable Φ effects on the turbulence chemistry interactions. Moreover, our approach also includes the effect of heat release due to premixed flame conditions in the vicinity of the triple point (where $G=0$ and $Z=Z_{st}$, see Section II.B and Figure 1).

The results in Figure 12 are for a reacting simulation with stoichiometric ratios of 0.65 and 0.85 for the lower and upper channels, respectively. For these values of the stoichiometric ratio, the laminar flame velocities, normalized by the bulk flow average velocity, are 0.005 and 0.022, respectively. Since the turbulent flame velocity is proportional to the laminar value for similar turbulence intensities, there are larger values for the flame propagation speed on the upper side of the combustion chamber compared to the lower side. The average flame

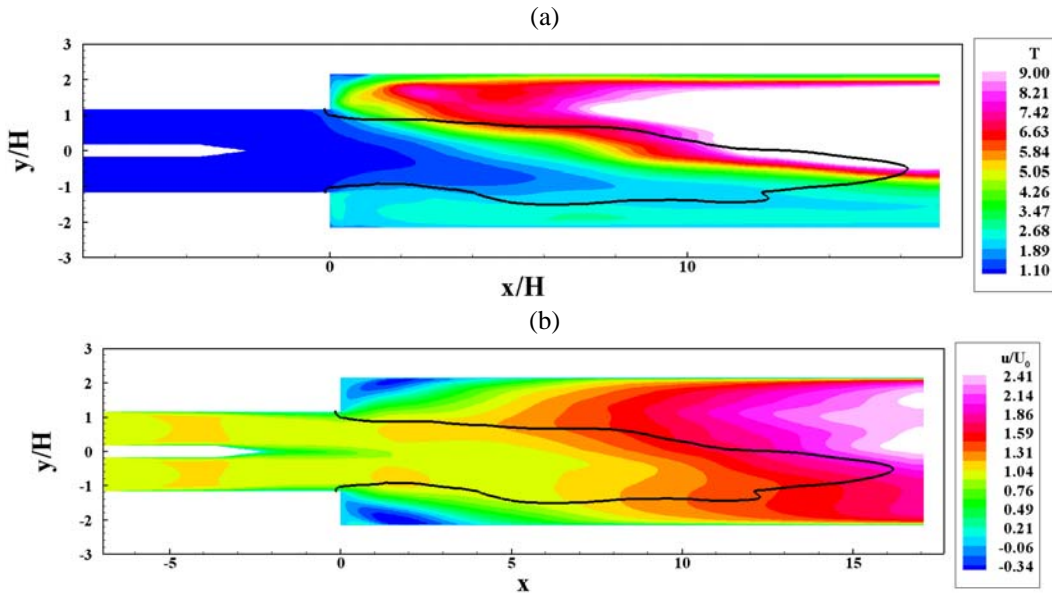


Figure 12 Snapshots of normalized time-averaged fields for the lean dump combustor: (a) temperature, (b) streamwise velocity component. The results correspond to a reacting simulation with variable equivalence ratio values: 0.65 for the lower inlet channel and 0.85 for the upper inlet channel.

location in Figure 12 is slanted towards the lower side and is in qualitative agreement with the results of Duchamp de Lageneste and Pitsch.⁶ The tip of the flame in the current simulations is located further downstream compared to the results of Duchamp de Lageneste and Pitsch.⁶ This is due to a lower stoichiometric ratio that was used in the present study.

The mixture on the upper inlet channel corresponds to a fuel-to-oxidizer ratio that is closer to the stoichiometric value compared to the lower channel. This results in larger heat release rates and higher temperatures, in Figure 12(a), for the upper side of the combustion chamber compared to the lower side. Since the flow is confined, the volumetric expansion leads to larger streamwise velocities on the upper side compared to the lower side.

In order to determine the effects of heat release on the flow field, the transverse profiles of the axial velocity component for the non-reacting and reacting simulations are compared with the experimental data in 3. Very good agreement can be observed for the non-reacting results in 3(a). The reacting results in 3(b) also show good agreement and exhibit the flow acceleration observed in Figure 12(b) for the profiles corresponding to $x/W=1.65$ and $x/W=3.62$. At $x/W=6.25$, the magnitude of the axial velocities on the upper side of the combustion chamber is slightly smaller for the numerical simulation compared to the experiment. The cause for this difference is still under investigation.

IV. Conclusions

In this paper, we further develop our combined level-set/mixture fraction approach for predicting truly unsteady, partially-premixed flame configurations, by re-evaluating our original procedures and providing further validations to re-affirm the accuracy of those procedures. The compressible flow solver incorporates high-order spatial and time differencing techniques coupled with a consistent high-order overset procedure to permit the analysis of realistic problems, which usually have very complex geometries. The coupling between chemical reaction and the flow field

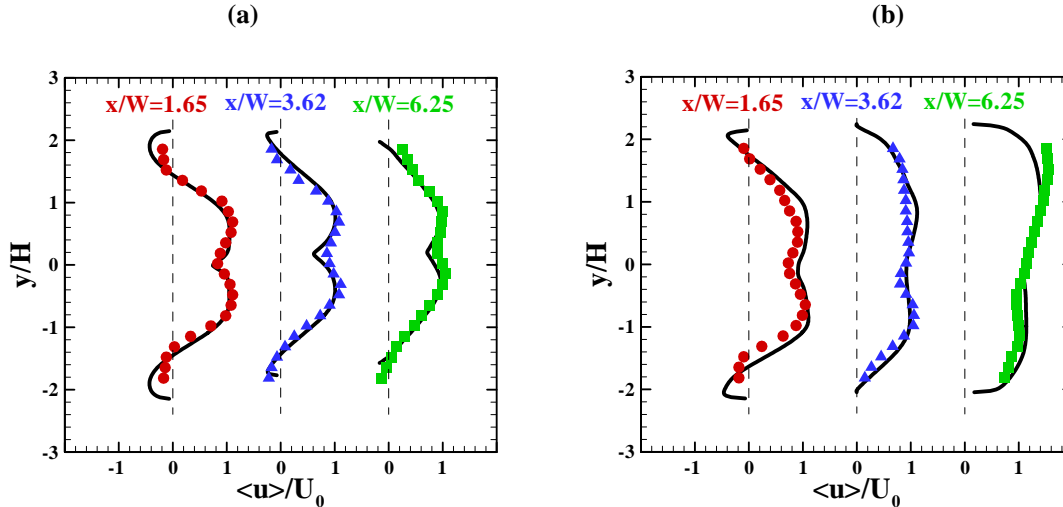


Figure 13 Comparison of the axial velocity profiles at several locations, x/W , downstream of the channel expansion: (a) non-reacting simulation and (b) reacting simulation. The solid lines correspond to the numerical simulations and the symbols to the experimental data. The vertical dashed lines correspond to zero levels at the corresponding axial locations. Here, $W=2.329H$ is the width of the channel where the upper and the lower streams are mixed right before the expansion.

is achieved through a level-set flamelet formulation for premixed regimes, augmented by a mixture fraction approach to account for variations in the equivalence ratio of the combustible mixture.

The above numerical approach is validated through comparisons with experimental data and results from previous numerical studies by other authors. The lean, premixed dump combustor is used to test the ability of the combined level-set/mixture fraction approach to capture the variable equivalence ratio for premixed configurations.

Acknowledgments

The author is grateful to Dr. Cosmin Safta, who carried out most of the calculations, to Drs. Xiaodan Cai and Ken Alabi for their input, to Tayo Ladeinde for generating the engine combustor grid, and to TTC Technologies, Inc. for permission to publish the work.

References

- ¹ Williams, F. A., "Turbulent Combustion," *The Mathematics of Combustion*, edited by J. Buckmaster, pp. 97-131, 1985.
- ² Peters, N., *Turbulent Combustion*, Cambridge University Press, 2000.
- ³ Pitsch, H. and Duchamp de Lageneste, L., "Large-Eddy Simulation of Premixed Turbulent Combustion Using a Level-Set Approach," *Proceedings of the Combustion Institute*, Vol. 29, pp. 2001-2008, 2002.
- ⁴ Pitsch, H., "A Consistent Level Set Formulation for Large-Eddy Simulation of Premixed Turbulent Combustion," *Combustion and Flame*, Vol. 143, pp. 587-598, 2005.
- ⁵ Huang, Y., Sung, H.-G., Hsieh, S.-Y., and Yang, V., "Large-Eddy Simulation of Combustion Dynamics of Lean-Premixed Swirl-Stabilized Combustor," *Journal of Propulsion and Power*, Vol. 19, No. 5, pp. 782, 2003.
- ⁶ Duchamp de Lageneste, L., and Pitsch, H., "Progress in Large-Eddy Simulation of Premixed and Partially-Premixed Turbulent Combustion," Center for Turbulence Research, Annual Research Briefs, pp. 97-107, 2001.
- ⁷ Lele, S. K., "Compact Finite Differences with Spectral-Like Resolution," *Journal of Computational Physics*, Vol. 103, No. 1, pp. 16-42, 1992.
- ⁸ Shu, C.-W., "Essentially Non-Oscillatory and Weighted Essentially Non-Oscillatory Schemes for Hyperbolic Conservation Laws," ICASE Report No. 97-65, November 1997.
- ⁹ Beam, R. M., and Warming, R. F., "An Implicit Factored Scheme for the Compressible Navier-Stokes Equations," *AIAA Journal*, Vol. 16, No. 4, pp. 393-402, 1978.
- ¹⁰ Safta, C., Alabi, K., Ladeinde, F., and Cai, X., "Level-Set Flamelet/Large-Eddy Simulation of a Premixed Augmentor Flame Holder," AIAA Paper 2006-0156, 2006.
- ¹¹ Safta, C., Alabi, K., and Ladeinde, F., "Comparative Advantages of High-Order Schemes for Subsonic, Transonic, and Supersonic Flows," AIAA Paper 2006-0299, 2006.
- ¹² Fye, D. J., "Economical Evaluation of Runge-Kutta Formulae," *Mathematics of Computation*, Vol. 20, No. 95, pp. 392-398, 1966.

- ¹³Harten, A., Engquist, B., Osher, S., and Chakravarthy, S., "Uniformly high order essentially non-oscillatory schemes, III," *Journal of Computational Physics*, Vol. 71, pp. 231-303, 1987.
- ¹⁴Shu, C.-W., "Efficient Implementation of Essentially Non-Oscillatory Shock Capturing Schemes," *Journal of Computational Physics*, Vol. 77, pp. 439-471, 1988.
- ¹⁵Shu, C.-W., "Efficient Implementation of Essentially Non-Oscillatory Shock Capturing Schemes, II," *Journal of Computational Physics*, Vol. 83, pp. 32-78, 1989.
- ¹⁶Sussman, M., Smereka, P., and Osher, S., "A Level Set Approach for Computing Solutions to Incompressible Two-Phase Flows," *Journal of Computational Physics*, Vol. 119, pp. 146-159, 1994.
- ¹⁷Russo, G., and Smereka, P., "A Remark on Computing Distance Functions," *Journal of Computational Physics*, Vol. 163, pp. 51-67, 2000.
- ¹⁸Spalart, P.R., and Allmaras, S.R., "A One-Equation Turbulence Model for Aerodynamic Flows," AIAA Paper 92-0439, 30th Aerospace Sciences Meeting & Exhibit, January 6-9, 1992.
- ¹⁹Cook, A.W., and Riley, J.J., "A Subgrid Model for Equilibrium Chemistry In Turbulent Flows," *Physics of Fluids*, Vol. 6, pp. 2868, 1994.
- ²⁰Smith, G. P., Golden, D. M., Frenklach, M., Moriarty, N. W., Eiteneer, B., Goldberg, M., Bowman, C. T., Hanson, R. K., Song, S., Gardiner, W. C., Lissianski, V. V., and Qin, Z., http://www.me.berkeley.edu/gri_mech [cited June 10, 2006].
- ²¹Besson, M., Bruel, P., Champion, J.L., and Deshaies, B., "Inert and Combusting Flows Developing over a Plane Symmetric Expansion: Experimental Analysis of the of the Main Flow Characteristics," AIAA Paper 99-0412, 1999.